Observations of Torsion on Bowed Strings

Robert Mores

HAW Mediencampus Finkenau, 22081 Hamburg, E-Mail:Robert.Mores@haw-hamburg.de

Abstract

Translational and torsional vibrations on bowed strings are well investigated, leaving the torsion with the less important role. Present models and simulations of the stick-slip interaction gain fidelity while incorporating limited bow hair elasticity, string stiffness, or bow width, but they do not explain some recent observations of collaboration between translational and torsional vibrations on the string. Torsion is measured on both sides of the bow contact point for a variety of bridge-bow distances on a cello string. Torsional vibrations decline over the course of the stick phase but then regain strength when the next release comes near. Structural and timing analyses suggest that differential bow slipping is causing such grow, putting the earlier concept of Schelleng ripples under question.

I. Introduction

In bowed string motion not only transverse waves but also torsional waves are excited due to the tangentially applied force at the surface of the string. String torsion is generally believed to have little impact on sound. Torsion is nevertheless believed to have a stabilizing effect on periodic bowed-string motion (Woodhouse, 1994). Torsion has therefore played a role in models and simulations of bowed strings.

The concept of the Schelleng ripples follows the argument that a wave arriving from the nut cannot because of its rounded corner immediately release the string from the bow (Schelleng, 1973). During the finite time it takes to build up the necessary threshold force the wave is reflected. Reflections from the bow travel to the nut and return again to the bow, arriving there just before the next release. In his bridge force recordings Schelleng observed that the ripple grows in the vicinity of an upcoming release. His explanation is that the individual ripple last to the instant of release is the one arising from the most recent wave reflection while the last but one ripple is the one arising from the last but one Helmholtz cycle, and so on. The last but one ripple experienced one additional cycle of reflections and associated damping and therefore has a smaller amplitude. The ripple diminishes over time, and only the timely sequence of their appearance evokes the impression of a growing ripple. The timely schematic of such occurrences is illustrated in Fig. 1a (McIntyre et al., 1981, Fig. 8). The youngest ripple relative to an upcoming release is denoted with the number 1 and the second youngest ripple is denoted with the number 2 in Fig. 1a.

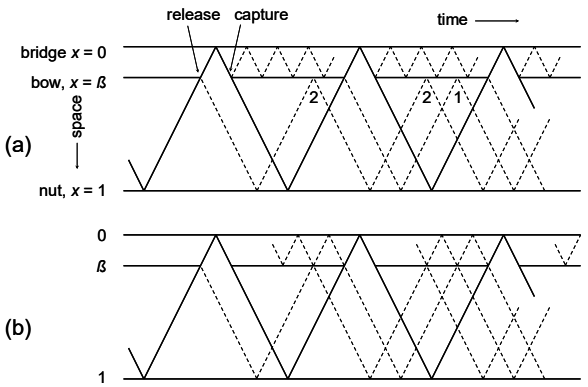

FIG. 1. Path of a Helmholtz corner in the space-time diagram. Heavy lines at bridge and nut indicate reflecting barriers, likewise the bow at position β in times of sticking. Paths of primary (──) and secondary (---) waves. (a) Principle of declining bridge-sided reflections at the beat of the recent stick-slip action and principle of nut-sided younger (1) versus older (2) Schelleng ripples, reproduced from McIntryre et al. (1981). (b) Observation in this study with bridge-sided reflections in phase with upcoming releases.

Another concept is that of limited bow width and the consequent differential slipping. Pitteroff and Woodhouse (1998, Part II) modelled the contact area across the bow width. The given width of a bundle of bow hairs in contact with the string suggests that there is no such concerted stick-slip action as ordinarily anticipated since the string, in conjunction with its gradual movement during sticking, also gradually changes its angle relative to the bow. The geometry of string movement therefore implies a displacement and a quasi-static force (Pitteroff and Woodhouse, 1998, Part II, Fig. 3).

The schematic in Fig. 2 qualitatively reproduces results from simulations. Within each complete Helmholtz cycle, i.e. an alternating slip and a stick across the entire width of the bow, there are interim slips along parts of the contact area, somewhat stronger at the inner edge of the bow hair.

FIG. 2. Multiple differential slipping in the course of fundamental stick-slip cycles. Results extracted from simulations on limited bow width (Pitteroff and Woodhouse, 1998, Part II), indicating that differential slipping occurs at the inner edge, on the bridge side.

II. Measurement and analysis

A cello steel G-string mounted on a monochord is bowed with a real bow. The string termination employs material of specific resistance. The material used here is a 4 mm thin layer of felt with a steel pin to support the string, with the measured resistance $R = 939 \pm 13$ kg/s (Mores, 2017).

The cello G string made of steel is a Pirastro Chromcor medium string with properties according to Table 1, most of which are measured. It is tuned to the nominal 98.0 ± 0.1 Hz at length l = 0.68 m.

TABLE 1. Properties of the Pirastro Chromcor Medium cello G string when tuned to 98 Hz.

core material		steel
mass per unit length	g/m	6.15
Diameter	mm	1.19
nominal tension	N	121
transverse wave speed v_{tra}	m/s	133
transverse wave impedance Z_0	Kg/s	0.93
torsional fundamental frequency	Hz	543
torsional wave speed v_{tor}	m/s	738

String velocity and torsional angular velocity are captured by electric coils. A pickup according to a Gibson patent (Isvan, 2002) is located directly underneath the bow contact point to capture string velocity. Torsional angular velocity is captured by a fine wire loop glued laterally to a few centimeters of the string, up one side and back down the other (Gillan and Elliott, 1989). The total mass load on the string is 4 mg, or 0.36% of the string's mass per unit length. Both velocity signals are integrated by a load amplifier to deliver displacement and angle.

A typical recording of an upstroke on the open G string is shown in Figure 4.

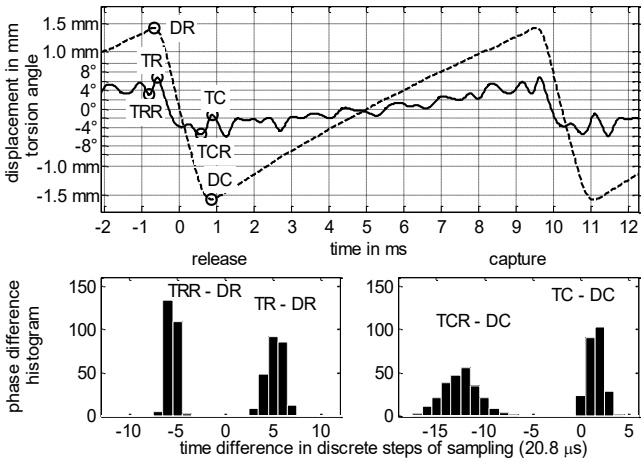

FIG. 4. String displacement (---), measured at the contact point, and torsion angle (——), measured 10 mm away from the contact point towards the bridge side, for an open cello G steel string when bowed at β = 80 mm with an upstroke, showing the average of eight consecutive cycles (top), with peaks of interest: release (DR) and capture (DC) of the string in the displacement signal, torsion during release (TR) and reverse torsion during release (TRR), as well as torsion during capture (TC) and reverse torsion during capture (TCR) in the torsion signal. Related histograms of the time differences between peaks of interest during release (bottom left) and capture (bottom right).

Zero on the time axis relates to the zero crossing of string displacement during slipping. Positive displacements and angles are directed towards bowing direction. The upper graph shows an overlay of eight consecutive periods, each triggered at its individual zero crossing. The center graph shows the average of these eight periods. The lower graph indicates the statistics of phase relations between torsion and displacement.

A few first observations: (i) torsion follows the general trend line of the periodic sawtooth because the displacement and the associated force applied to the string also causes quasi-static torsion, (ii) there is no regular torsional wave but there are short sections of harmonic torsional oscillation just before and after the slipping while the rest of the trace seems to be chaotic., (iii) the character of the torsion signal depends strongly on β but does not vary much with bow force or with bow velocity, (iv) the amplitude of torsional oscillation and therefore the associated ripple in the displacement trace grows while the release comes nearer.

In the graph, points of return for displacement and torsion are indicated. DR marks the point of return regarding the displacement during release action, and DC marks this for the capture action. TR corresponds to the point of return of torsion during the capture action, TC for the capture action. Both maxima represent torsional angles the direction of which agrees with the current bowing direction. TRR and TCR represent minima that directly precede these maxima with a direction reverse to bowing which might indicate slipping. Phase histograms indicate the time difference between maxima of torsion and displacement for 250 consecutive cycles, with bins given by the sampling rate of 48 kHz.

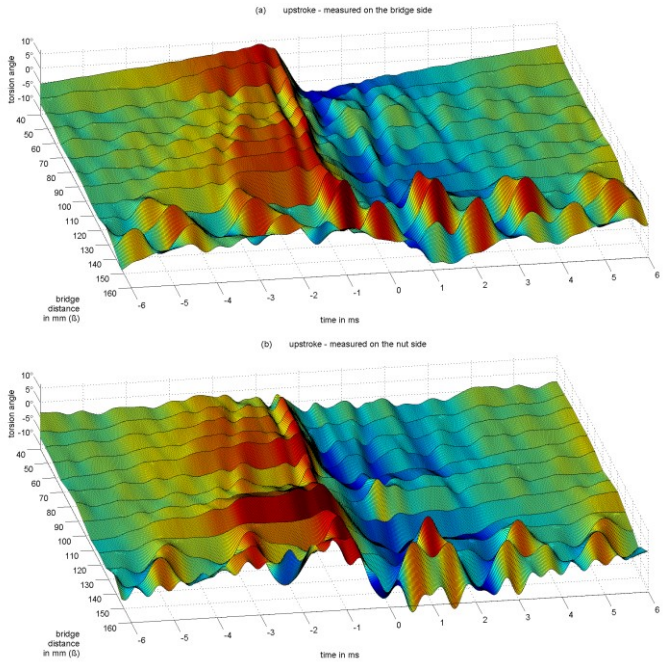

FIG. 3. Torsional vibration of a bowed open cello G-string on a monochord for varying β. Pickup position 10 mm away from the contact point towards (a) the bridge and (b) the nut. Reference at 0 ms is the zero-crossing of the respective displacement signal during release (not shown here).

Fig. 3 summarizes qualified raw data (upstrokes only). The total of 52 individual manual down- and upstrokes comes with varying bowing velocity and bow force. By visual inspection, there are similarities but also differences between bridge side and nut side. The structure follow rules in relation with β in the range from 40 mm to 120 mm, the

typical playing range. Within this range, the structure is more or less regular. Structure and the phase relations both systematically change only at β = 130 mm and above, when bowing at approximately β = 1/5 = 136 mm.

TABLE 2. Loop times of transverse and torsional waves on the open cello G string in relation to β.

β in mm	torsional wave loop time in ms between bow and		transverse wave loop time in ms between bow and	
	bridge	nut	bridge	nut
40	0.11	1.73	0.60	9.62
60	0.16	1.68	0.90	9.32
80	0.22	1.63	1.20	9.02
100	0.27	1.57	1.50	8.72
120	0.33	1.52	1.81	8.42

Note that the visible two to three steps prior to slipping correspond well to the loop-times of transverse waves on the bridge side, Table 2. The steps correspond to a Helmholtz motion for the fraction of the string determined by β, say a fractional Helmholtz motion (*f-HM*). Contrary to the expectation of damping, the impulses gain in strength with the advent of a release. Each reflection of transverse waves, or, each *f-HM* cycle, is accompanied by torsional motion. The torsional motion is identifiable by densely following positive and negative impulses. Torsional and transverse vibrations work together: each reflection of transverse waves is accompanied by a preceding stronger-than-usual reverse torsional motion. This reverse torsional motion comes from differential slipping.

Fig. 4 summarizes measured phase relations for the release section. In the top graph, Δ_{br} denotes the time difference between the turning points of the torsional and the transverse waves, measured at the bridge side during release, Δ_{br} = t(TR) - t(DR). Likewise, Δ_{brr} denotes the time difference between turning point of the torsional wave in reverse direction that precedes the turning point of the transverse wave, Δ_{brr} = t(TRR) - t(DR), measured at the bridge side as well. The upper middle graph summarizes the same phase relations, but measured at the nut side, Δ_{nr} = t(TR) - t(DR), and Δ_{nrr} = t(TRR) - t(DR). The histogram in the bottom left graph of Fig. 4 now translates to Δ_{br} = 20.8 µs · (5.2 ± 0.9) = 108 ± 19 µs for the upstroke at β = 80 mm, for instance.

Every entry represents the mean and the standard deviation of phase relations across 250 fundamental cycles, for each down- and upstroke at each position. Bow force and bow velocity are *not* set to a single predefined value but the dynamic range purposely alters by a factor of minimum two for all strokes.

Theres is evidence for three statements:

(i) *Pre-release reverse torsion*: Δ_{brr} is always roughly 100 µs for β in the range from 50 to 120 mm, and the standard deviation is always less than 18 µs. Therefore, there is a specific phase relation between the torsional waves only depending on the string properties and the tuning.

(ii) *Distinction on the bridge side*: The standard deviation is larger for almost all observations on the nut side as compared to the bridge side. This observation might suggest that action or synchronizing events are more likely to happen on the string section at the bridge side while the string section at the nut side follows. Likewise, Figs. 5a shows a more regular temporal structure than 5b.

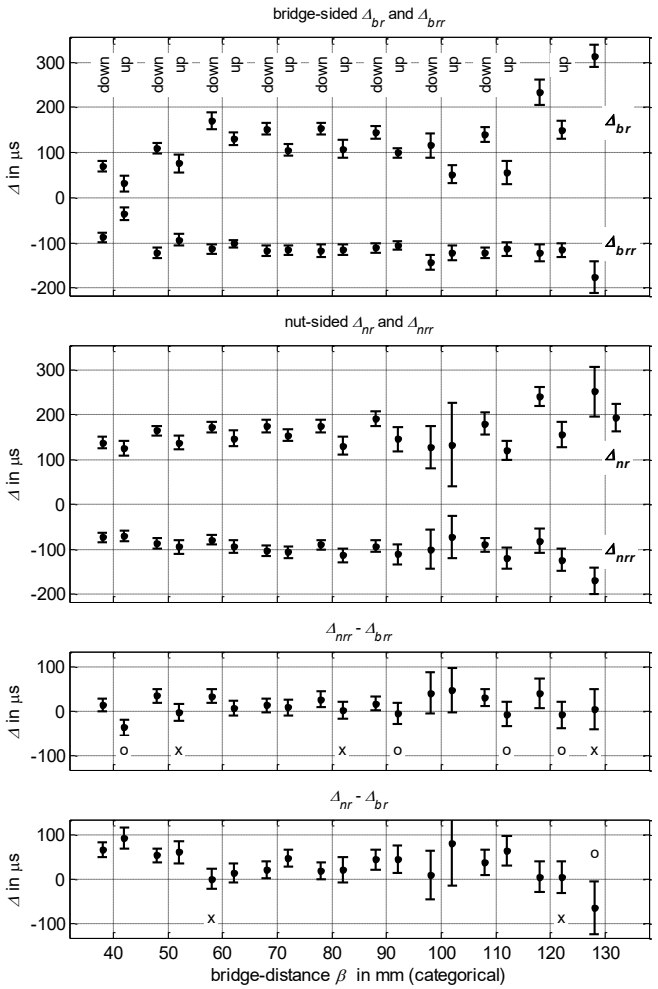

FIG. 4. Phase relations between peaks of interest in the course of bow release on an open cello G string. For the individual time differences Δ in the upper two graphs see text, peaks of interest are indicated in Fig. 4. By comparison of time differences Δ in the lower two graphs peaks on the bridge side appear always significantly earlier than peaks on the nut side unless where indicated: (×) no significance, (○) opposite direction, peaks appear earlier on nut side.

(iii) *Prior action on the bridge side*: the lower center graph in Fig. 9 represents the difference between Δ_{nrr} - Δ_{brr}. This difference indicates whether the reverse torsion happens earlier at the bridge side or at the nut side. The standard deviation slightly increases for the calculated difference at each β due to the two given distributions. In almost all cases, the reverse torsion happens earlier at the bridge side by typically 10 to 25 µs. This time difference suits the fact that the travel time of torsional waves from the inner edge of the bow to the bridge sided pickup is 14 µs shorter than the travel time from inner edge to the nut-sided pickup. This earlier action is significant as suggested by the rejected null hypothesis for the distributions of Δ_{nrr} and Δ_{brr}, at 5 % significance. There are only three exceptions where the null hypothesis is not rejected, indicated by 'x' in the graph. Four other exceptions indicate a faster action at the nut side, indicated by 'o' in the graph.

Before reasoning how the transverse wave that arrives at the outer edge could possibly co-determine the differential slipping happening at the inner edge there is another even more puzzling question: how come the timing of the *f-HM* cycles always coincides with the upcoming release action? If it was the Schelleng ripple, the synchronization would come from previous cycles, see upper graph in Fig. 1, and the question would be answered. However, it is evident that (i) the cooperation of reflected transverse waves and differential slipping is the fundamental action, not the Schelleng ripple, (ii) this action takes place on the bridge side, (iii) the growing ripple comes from the force that increases during the course of the cycle, *not* supporting the argument of younger versus older Schelleng ripples.

There might be a single answer to both questions. The transverse wave which, reflected from the bridge, forms the main cycle, and the transverse wave of the Schelleng ripple have the same direction on arrival at the outer edge. So whatever a reflected transverse wave can do for the main cycle it can also do for intermediate *f-HM* cycles. The argument now is that the *f-HM* cycle gets synchronized with the returning Schelleng ripples. Both, the *f-HM* cycle and the difference between a total loop-time and the fractional loop-time of a Schelleng cycle are of same length anyway and therefore likely to synchronize, see Figs. 1a and 1b. Observations suggest a synchronization of the *f-HM* cycles, which are driven on the bridge side, with the Schelleng cycles, which, if they exist, reverberate on the nut side.

To summarize this section, (i) releases are always preceded by a reverse torsional motion at the contact point at distinct times, (ii) the reverse torsional motion is caused by differential slipping, because the relevant torsional impulses appear earlier at the bridge side compared to the nut side, (iii) the phase of the *f-HM* cycles driven by differential slipping is not derived from a recent capture, as believed so far, but aligns perfectly with an upcoming release, Fig. 1b, (iv) therefore, the sequence of Schelleng ripples returning at the outer edge is believed to synchronize the *f-HM* cycles, the action of which still strictly takes place at the inner edge.

IV. Recapitulation and discussion

Following observations are evident and should be reproducable without problems:

(i) The release is always preceded by a strong reverse torsional motion. The span between these two events is distinct, the standard deviation is always less than 18 µs across the entire playing range for the open cello G string. This phase relation does not alter with β.

(iii) The release is synchronized with the final of a sequence of *f-HM* cycles. These cycles are generated on the bridge side as can be proofed by the phase relations of bridge-sided versus nut-sided torsions, across the playing range. These cycles are believed to be caused by differential slipping.

(iii) Across the playing range, *f-HM* cycles are always accompanied synchronously by a pair of a reverse and a forward torsional motion. This also relates to differential slipping, since the partial release of the string will not only cause fractional backward slipping but also fractional reverse torsion, since the applied and then released forces work for both.

One of the main findings is that the concept of Schelleng ripple is under question. The growth of these ripples was explained so far with the older vs. younger argument resulting from the reverse-order-of-appearance at the contact point, Fig. 1a. However, when comparing the bridge side with the nut side, the timing analysis proofs that the action is happening at the bridge side. The growth is plausible, since differential slipping gains strength during the course of the fundamental cycle as the applied forces increase with displacement. The temporal patterns show that the periodical slipping is in line with the upcoming release and not with the past capture, Fig. 1b. Observations and arguments calls the concept of Schelleng ripples into question.

Different slipping can be confirmed. Earlier descriptions related to differential slipping appear comply with present observations. There are indeed strong torsional vibrations generated during the course of a fundamental cycle which can only come from the action of differential slipping. And indeed the action takes place at the inner edge of the bow.

V. Conclusions

The concept of differential slipping can be confirmed, however, the concept of Schelleng ripples cannot be confirmed. The evidence comes from measured phase relations. The initiative for the fractional Helmholtz cycle is clearly coming from actions at the inner edge, on the bridge side, while Schelleng ripples are nut-sided.

References

Gillan, F. S., and Elliott, S. J. (**1989**). "Measurement of the torsional modes of vibration of strings on instruments of the violin family," J. of Sound and Vibration, **130**(2), 347–351.

Isman, O. K. (**2002**). "Polyphonic guitar pickup for sensing string vibrations in two mutually perpendicular planes," Patent US 6392137.

Mansour, H., Woodhouse, J., and Scavone, G. P. (**2016**). "Enhanced wave-based modelling of musical strings. Part 2: Bowed strings," Acta Acustica united with Acustica, **102**(6), 1094–1107.

McIntyre, M. E., Schumacher, R. T., and Woodhouse, J. (**1981**). "Aperiodicity in bowed-string motion," Acta Acustica united with Acustica, **49**(1), 13–32.

Mores, R. (**2017**). "Complementary empirical data on minimum bow force," J. Acoust. Soc. Am., **142**(2), 728–736.

Pitteroff, R., and Woodhouse, J. (**1998**). "Mechanics of the contact area between a violin bow and a string. Part II: Simulating the bowed string," Acta Acustica united with Acustica, **84**(4), 744–757.

Schelleng, J. (**1973**). "The bowed string and the player," J. Acoust. Soc. Am. **53**, 26–41.

Woodhouse, J. (**1994**). "On the stability of bowed string motion," Acta Acustica united with Acustica, **80**(1), 58–72.